Ground state of $N=Z$ doubly closed shell nuclei in correlated basis function theory

A. Fabrocini,[1] F. Arias de Saavedra,[2] G. Co',[3] and P. Folgarait[4,1]
[1]*Istituto Nazionale di Fisica Nucleare, Dipartimento di Fisica, Università di Pisa, I-56100 Pisa, Italy*
[2]*Departamento de Fisica Moderna, Universidad de Granada, E-18071 Granada, Spain*
[3]*Istituto Nazionale di Fisica Nucleare, Dipartimento di Fisica, Università di Lecce, I-73100 Lecce, Italy*
[4]*Centro Ricerche e Sviluppo, Gruppo Lucchini, I-57025 Piombino, Italy*
(Received 6 October 1997)

The ground state properties of $N=Z$ doubly closed shell nuclei are studied within correlated basis function theory. A truncated version of the Urbana v_{14} realistic potential, with spin, isospin, and tensor components, is adopted, together with state-dependent correlations. Fermi hypernetted chain integral equations are used to evaluate the density, distribution function, and ground state energy of ^{16}O and ^{40}Ca. The nuclear matter single operator chain approximation is extended to finite nuclear systems, to deal with the noncommuting part of the correlation operators. The results favorably compare with variational Monte Carlo estimates, when available, and provide a first substantial check of the accuracy of the cluster summation method for state-dependent correlations. We achieve in finite nuclei a treatment of noncentral interactions and correlations having, at least, the same level of accuracy as in nuclear matter. This opens the way for a microscopic study of the medium heavy nuclei ground state using present day realistic Hamiltonians. [S0556-2813(98)00104-6]

PACS number(s): 21.60.Gx, 21.10.Dr, 27.20.+n, 27.40.+z

I. INTRODUCTION

It is now a largely accepted fact that the wave function of strongly interacting nuclear systems shows large deviations from independent particle models (IPM's). These effects may be ascribed to the presence of correlations between the nucleons, coming from the nuclear interaction. Several nucleon-nucleon (NN) potentials are presently available, all of them fitting the deuteron and the NN scattering data up to energies of several hundred MeV. However, their complicated structure and dependence on the state of the interacting nucleons has severely hindered the achievement of realistic, *ab initio* studies of most of the nuclear systems.

The situation is satisfactory for light nuclei. Faddeev [1], Green function Monte Carlo (GFMC) [2], and correlated hyperspherical harmonics expansion (CHHE) [3] theories solve exactly the Schrödinger equation in the $A=3,4$ cases for realistic Hamiltonians. Recently GFMC theory has been extended up to $A=7$ [4]. Moreover, these theories (particularly Faddeev and CHHE) are now successfully used to study low energy reactions involving three nucleons [5]. Light nuclei properties may be also described by variational Monte Carlo (VMC) [6] methods. If the spanned variational wave function space is large enough, then the description provided by a variational approach is quite accurate (even if not exact). One of the major advantages of the VMC method is its larger flexibility, resulting in the possibility of an extension to heavier nuclei, such as ^{16}O [7].

At the opposite asymptotic side of the nuclear table, infinite nuclear matter has attracted the attention of researchers, as it is thought to be a reliable model for the interior of nuclei. High density neutron matter and asymmetric nuclear matter are also objects of intensive investigations because of their astrophysical relevance. The equations of state (EOS) of infinite systems of nucleons have been studied, in nonrelativistic approaches and using realistic interactions, either by Brueckner-Bethe-Goldstone (BBG) perturbation theory [8,9] or correlated basis function (CBF) theory [10,11]. These theories give consistent results at densities close to the nuclear matter empirical saturation density ($\rho_{\rm nm}=0.16$ fm^{-3}), whereas large discrepancies appear at higher density values. A question still to be answered is the convergence of the hole line expansion, on which BBG theory is based, in the case of a continuous choice for the auxiliary potential. Recent BBG results are all obtained within the two-hole line approximation [9]. Attempts are under way to evaluate the three-hole line contribution [12].

CBF nucleonic EOS give a good microscopic description of nuclear matter around saturation and provide a description of the neutron star structure in agreement with current observational data [10]. Moreover, nuclear matter dynamical quantities, such as electromagnetic responses [13,14] and one-body Green functions [15], may be accurately addressed by CBF-based perturbative expansions.

Medium-heavy nuclei still lack microscopic studies with realistic Hamiltonians. In a series of papers, the authors succeeded in extending CBF approaches to the ground state of doubly closed shell nuclei (both in ls and jj coupling) with semirealistic, central interactions and simple two-body correlations, depending only on the interparticle distances and, at most, on the isospin of the correlated pair [16–18]. Nuclei ranging from ^{4}He to ^{208}Pb were investigated in those papers by model Hamiltonians. The aim of the present work is to extend those studies to NN interactions and correlations containing spin, isospin, and tensor components. We shall consider ^{16}O and ^{40}Ca nuclei, having doubly closed shells in ls coupling. We shall adapt to these systems the cluster summation technique, used in symmetric nuclear matter for state-dependent correlations. Modern interactions have also important spin-orbit parts, which are not included in the present treatment, as well as other remaining components. They will be the objects of future works. A first order cluster expansion has been recently used to study the influence of state-

dependent correlations on the one-body density matrix of closed shell nuclei [19].

Our work is carried out in the framework of a nonrelativistic description of the atomic nucleus with Hamiltonians of the type

$$H=\frac{-\hbar^2}{2m}\sum_i \nabla_i^2+\sum_{i<j} v_{ij}+\sum_{i<j<k} v_{ijk}. \tag{1}$$

The two- and three-nucleon potentials v_{ij} and v_{ijk} are determined at large interparticle distances by meson exchange processes. The intermediate and short distance regimes are usually treated in a semimicroscopic or purely phenomenological fashion. We shall use a truncated version of the realistic Urbana v_{14} model (U14) of the NN interaction [20] but we shall not consider three-nucleon potentials. We shall also present results for the central semirealistic interaction $S3$ by Afnan and Tang, v_{S3} [21], which reproduces the s-wave two-body scattering data up to roughly 60 MeV and gives values of the ground state properties of light nuclei and of nuclear matter close to those obtained by more realistic interactions. The $S3$ potential has been supplemented in the odd channels, where it is not defined, with the repulsive term of the even channels.

The full U14 model has the following parametrization:

$$v_{14,ij}=\sum_{p=1,14} v^p(r_{ij})O_{ij}^p, \tag{2}$$

with

$$O_{ij}^{p=1,14}=[1,\sigma_i\cdot\sigma_j,S_{ij},(\mathbf{L}\cdot\mathbf{S})_{ij},L^2,L^2\sigma_i\cdot\sigma_j,(\mathbf{L}\cdot\mathbf{S})_{ij}^2]\otimes[1,\tau_i\cdot\tau_j], \tag{3}$$

$S_{ij}=(3\hat{r}_{ij}\cdot\sigma_i\hat{r}_{ij}\cdot\sigma_j-\sigma_i\cdot\sigma_j)$ being the usual tensor operator. In the v_6 truncation we shall retain components up to the tensor ones, thus neglecting the spin-orbit and higher terms ($p>6$). $S3$ does not have the $p=3,6$ tensor parts.

The ground-state-correlated A-body wave function is given, in our CBF approach, by

$$\Psi(1,2,\ldots,A)=\left(\mathcal{S}\prod_{i<j} F_{i,j}\right)\Phi(1,2,\ldots,A), \tag{4}$$

where a symmetrized product of the two-body correlation operators F_{ij} acts on the mean field state, $\Phi(1,2,\ldots,A)$, taken as a shell model wave function built up with $\phi_\alpha(i)$ single particle wave functions. Consistently with the interaction, F_{ij} is chosen of the form

$$F_{ij}=\sum_{p=1,6} f^p(r_{ij})O_{ij}^p. \tag{5}$$

The tensor components of F_{ij} are omitted in the $S3$ case.

The $f^p(r)$ functions contain a set of variational parameters determined by minimizing the ground state expectation value of the Hamiltonian, $\langle H\rangle=\langle\Psi|H|\Psi\rangle/\langle\Psi|\Psi\rangle$. The many-body integrals needed for the evaluation of $\langle H\rangle$, as well as of the expectation value of other operators, could be in principle sampled by Monte Carlo (MC) techniques. However, MC methods for realistic, state-dependent models can be efficiently used only in light nuclei. An alternative approach, suitable to heavier systems, is the cluster expansion and Fermi hypernetted chain (FHNC) [22] integral equations. The FHNC equation allows for summing infinite classes of Mayer-like diagrams and it has been widely applied to both finite and infinite interacting systems with state-independent (or Jastrow) correlations.

The strong state dependence of F_{ij}, needed for a realistic description of nuclear systems and resulting in the noncommutativity of the correlation operators prevents the development of a complete FHNC theory for the correlated wave function of Eq. (4) and forces one to look for suitable approximations. The single operator chain (SOC) approximation presented in Ref. [23] [hereafter referred to as PW] for the operatorial correlations, in conjunction with a full FHNC treatment of the scalar part, provides an apparently accurate description of infinite nuclear and neutron matter [10]. The FHNC and SOC treatments are thought to effectively include the contribution of many-body correlated clusters. However, no exact check for the FHNC and SOC treatments is presently available in nuclear matter, apart from the evaluation of some additional classes of diagrams. The estimated accuracy in the ground state energy has been set to less than 1 MeV at saturation density [24,10].

We shall use FHNC-SOC theory to study the ground state of ^{16}O and ^{40}Ca described by the correlated wave function (4). The ^{16}O results will be compared with the MC calculations of Ref. [7], where the scalar part of the correlation is exactly treated by the MC method, and the contribution of the operatorial components ($p>1$) is approximated by considering up to four-body cluster terms. Higher order contributions are then extrapolated.

The plan of the paper is the following: In Sec. II we present the FHNC-SOC theory for the one-body density and the two-body distribution function; the ground state energy calculation is discussed in Sec. III; the results obtained for ^{16}O and ^{40}Ca are presented and discussed in Sec. IV; conclusions and future perspectives are given in Sec. V.

II. FHNC-SOC THEORY FOR FINITE SYSTEMS

In discussing the FHNC-SOC approach to the one- and two-body densities, $\rho_1(\mathbf{r}_1)$ (OBD) and $\rho_2^p(\mathbf{r}_1,\mathbf{r}_2)$ (TBD), defined as

$$\rho_1(\mathbf{r}_1)=\left\langle\sum_i \delta(\mathbf{r}_1-\mathbf{r}_i)\right\rangle \tag{6}$$

and

$$\rho_2^p(\mathbf{r}_1,\mathbf{r}_2)=\left\langle\sum_{i\neq j} \delta(\mathbf{r}_1-\mathbf{r}_i)\,\delta(\mathbf{r}_2-\mathbf{r}_j)O_{ij}^p\right\rangle, \tag{7}$$

we shall heavily rely on the formalism developed in PW and in Ref. [16], denoted as CO1 hereafter. Most of the quantities we shall introduce and use in this section are described in those papers and will not be discussed here. Moreover, the various $p=1,6$ components of the correlation (and other quantities) will be often referred to as $c(p=1)$ and, with an obvious notation, as σ, τ, and t (tensor).

In Jastrow FHNC theory, the TBD is written in terms of the scalar correlation $f^c(r)$ and of the *nodal* (or *chain*) and *elementary* (or *bridge*) functions $N_{xy}(\mathbf{r}_1,\mathbf{r}_2)$ and $E_{xy}(\mathbf{r}_1,\mathbf{r}_2)$, representing the sums of the diagrams having those topological structures, respectively. The diagrams are further classified according to the exchange character (xy) of the external points (1,2) $x(y)=d,e$ with $d=$direct and $e=$exchange. (cc) $(c=$cyclic) diagrams are also present, whose external points are joined by a single, nonclosed exchange loop (see CO1 for more details).

When operatorial correlations are introduced, the nodal functions become $N^p_{xy}(\mathbf{r}_1,\mathbf{r}_2)$, where p denotes the state dependence associated with the function. A complete FHNC treatment for the full, state-dependent TBD is not presently possible, and so a SOC approximation was introduced in PW. It consists of summing $p>1$ chains, where each link may contain just one operatorial element and central dressings at all orders. We recall that operatorial dependence comes also from the exchanges of two nucleons. In fact, to every exchange line forming a closed loop but one is associated the exchange operator $P_{ij}=-\Sigma_{q=c,\sigma,\tau,\sigma\tau}O^q_{ij}/4$.

The FHNC-SOC integral equations for $N^p_{xy}(\mathbf{r}_1,\mathbf{r}_2)$, with $x(y)=d,e$, are

$$N^p_{xy}(1,2)=\sum_{x'y'}\sum_{qr}\int d^3r_3\xi^{qrp}_{132}X^q_{xx'}(1,3)V^{qr}_{x'y'}(3)\times[X^r_{y'y}(3,2)+N^r_{y'y}(3,2)]. \tag{8}$$

The allowed $(x'y')$ combinations are dd, de, and ed, and the coordinate $\mathbf{r}_i$ is indicated as i. $V^{qr}_{x'y'}(3)$ are vertex corrections in $\mathbf{r}_3$ that will be discussed later; ξ^{qrp}_{132} are angular couplings given in PW [Eqs. (5.6)–(5.11)]. Actually, they were given only in the operatorial channels $(p,q,r>1)$. In the $p=1$ channel, the coupling function is one if $q=r=1$; otherwise it is zero. The $X^c_{xy}(1,2)$ links are defined in CO1, while, for $p>1$, we have

$$X^p_{dd}(1,2)=h^p(1,2)h^c(1,2)-N^p_{dd}(1,2), \tag{9}$$

$$X^p_{de}(1,2)=h^c(1,2)\{h^p(1,2)N^c_{de}(1,2)+[f^c(r_{12})]^2N^p_{de}(1,2)\}-N^p_{de}(1,2), \tag{10}$$

$$X^p_{ee}(1,2)=h^c(1,2)(h^p(1,2)[N^c_{de}(1,2)N^c_{ed}(1,2)+N^c_{ee}(1,2)]+[f^c(r_{12})]^2\{N^p_{ee}(1,2)+N^p_{de}(1,2)N^c_{ed}(1,2)+N^c_{de}(1,2)N^p_{ed}(1,2)-4[N^c_{cc}(1,2)-\rho_0(1,2)]^2\Delta^p\})-N^p_{ee}(1,2), \tag{11}$$

with

$$h^p(1,2)=f^c(r_{12})\{2\,f^p(r_{12})+f^c(r_{12})N^p_{dd}(1,2)\}, \tag{12}$$

$h^c(1,2)=\exp[N^c_{dd}(1,2)]$, and $\Delta^p=1$ for $p=c,\sigma,\tau,\sigma\tau$; otherwise it is zero. $\rho_0(1,2)$ is the IPM density matrix, given in CO1, $N^c_{cc}(1,2)$ is the central cc nodal function, given later, and $X^p_{ed}(1,2)=X^p_{de}(2,1)$. The FHNC/0 approximation (corresponding to setting to zero the elementary diagrams) has been assumed in the above equations. Its validity will be discussed in the results section.

For the cc-type nodals we have

$$N^p_{xx}(1,2)=\sum_{qr}\int d^3r_3\xi^{qrp}_{132}X^q_{cc}(1,3)V^{qr}_{cc}(3)\times[X^c_{cc}(3,2)+N^c_{xx}(3,2)+N^c_{\rho x}(3,2)]\Delta^r+\sum_{qr>1}\int d^3r_3\xi^{qrp}_{132}\Delta^qX^c_{cc}(1,3)V^{qr}_{cc}(3)\times[X^r_{cc}(3,2)+N^r_{xx}(3,2)+N^r_{\rho x}(3,2)], \tag{13}$$

$$N^p_{x\rho}(1,2)=\sum_{qr}\int d^3r_3\xi^{qrp}_{132}X^q_{cc}(1,3)V^{qr}_{cc}(3)\times[-\rho_0(3,2)+N^c_{x\rho}(3,2)+N^c_{\rho\rho}(3,2)]\Delta^r+\sum_{qr>1}\int d^3r_3\xi^{qrp}_{132}\Delta^qX^c_{cc}(1,3)V^{qr}_{cc}(3)\times[N^r_{x\rho}(3,2)+N^r_{\rho\rho}(3,2)], \tag{14}$$

$$N^{p=1}_{\rho\rho}(1,2)=\int d^3r_3[-\rho_0(1,3)]V^{11}_{cc}(3)N^c_{x\rho}(3,2)+\int d^3r_3[-\rho_0(1,3)][V^{11}_{cc}(3)-1]\times[-\rho_0(3,2)+N^c_{\rho\rho}(3,2)], \tag{15}$$

$$N^{p>1}_{\rho\rho}(1,2)=\sum_{qr}\int d^3r_3\xi^{qrp}_{132}[-\rho_0(1,3)\Delta^q]V^{qr}_{cc}(3)N^r_{x\rho}(3,2)+\sum_{qr}\int d^3r_3\xi^{qrp}_{132}[-\rho_0(1,3)\Delta^q]\times[V^{qr}_{cc}(3)-1]N^r_{\rho\rho}(3,2). \tag{16}$$

Again, $X^c_{cc}(1,2)$ is defined in CO1, and

$$X^{p>1}_{cc}(1,2)=h^p(1,2)h^c(1,2)[N^c_{cc}(1,2)-\rho_0(1,2)]+\{[f^c(r_{12})]^2h^c(1,2)-1\}N^p_{cc}(1,2). \tag{17}$$

The $x(\rho)$ subscript indicates that the external point is (not) reached by an X link, $N^p_{cc}=N^p_{xx}+N^p_{x\rho}+N^p_{\rho x}+N^p_{\rho\rho}$ and $N^p_{\rho x}(1,2)=N^p_{x\rho}(2,1)$.

Because in an exchange loop involving more than two nucleons only one of the exchanged pairs does not have any operatorial link from P_{ij} and in the spirit of the SOC approximation, the $f^{p>1}$ correlations appear once in the cc chains, just for that pair.

Single operator rings (SOR's) were also approximately included into the central chains in PW. SOR's are closed loops of operators having a nonzero C part. A product of operators can be expressed, by the Pauli identity, as the sum of a spin- and isospin-independent piece (the C part) and a remainder, linear in σ_i or τ_i. In nuclear matter, as well as in the nuclei we are considering (doubly closed shell nuclei in ls coupling), the spin-isospin trace of the remainder vanishes, leaving only the C part as the final contribution of the

product. An example is $O^{\sigma}_{12}O^{\sigma}_{23}O^{\sigma}_{31}$, having a C part of 3. SOR's contribute to $p=1$ chains and were introduced by PW in the definition of X^c_{xy}. A drawback of this approach is that touching SOR's, i.e., SOR's having a common vertex, are wrongly counted because commutators are neglected. For this reason, we do not follow PW and do not include SOR's in our treatment of N^c_{xy}. However, in one test case we have used the PW prescription to gauge the relevance of the missing contribution. The results will be presented later.

The OBD $\rho_1(\mathbf{r}_1)$ is computed following CO1. Its structure results in

$$\rho_1(\mathbf{r}_1)=\rho^c_1(\mathbf{r}_1)[1+U^{op}_d(\mathbf{r}_1)]+U^{op}_e(\mathbf{r}_1)C_d(\mathbf{r}_1), \quad (18)$$

with

$$\rho^c_1(\mathbf{r}_1)=[\rho_0(\mathbf{r}_1)+U^c_e(\mathbf{r}_1)]C_d(\mathbf{r}_1), \quad (19)$$

where $\rho_0(\mathbf{r}_1)=\Sigma_\alpha|\phi_\alpha(1)|^2$ is the IPM density, $C_d(\mathbf{r}_1)=\exp\{U^c_d(\mathbf{r}_1)\}$ and $U^c_{d(e)}(\mathbf{r}_1)$ are the central vertex corrections of CO1. They are solutions of two integral equations (A.19) and (A.20), given in the Appendix of that paper. These equations must be modified because of the presence of operatorial correlations by the substitutions $\xi_d(\mathbf{r}_2)\to\rho_1(\mathbf{r}_2)$ and $\xi_e(\mathbf{r}_2)\to[1+U^{op}_d(\mathbf{r}_2)]C_d(\mathbf{r}_2)$.

The SOC operatorial vertex corrections $U^{op}_{d(e)}(\mathbf{r}_1)$ are solutions of the equations

$$\begin{aligned}U^{op}_d(1)=&\sum_{p>1}A^p\int d^3r_2h^c(1,2)f^p(r_{12})\\&\times\{[f^p(r_{12})+f^c(r_{12})N^p_{dd}(1,2)]\rho^c_1(2)\\&+[f^p(r_{12})+2\,f^c(r_{12})N^p_{dd}(1,2)]N^c_{de}(1,2)C_d(2)\\&+f^c(r_{12})N^p_{de}(1,2)C_d(2)\},\end{aligned} \quad (20)$$

$$\begin{aligned}U^{op}_e(1)=&\sum_{p>1}A^p\int d^3r_2h^c(1,2)f^p(r_{12})\\&\times([f^p(r_{12})+2\,f^c(r_{12})N^p_{dd}(1,2)]\{N^c_{ed}(1,2)\rho^c_1(2)\\&+[N^c_{de}(1,2)N^c_{ed}(1,2)+N^c_{ee}(1,2)]C_d(2)\}\\&+2\,f^c(r_{12})\{N^p_{ee}(1,2)C_d(2)+N^p_{ed}(1,2)\\&\times[\rho^c_1(2)+N^c_{de}(1,2)C_d(2)]\})+U^{op}_c(1),\end{aligned} \quad (21)$$

where $A^{p=1,6}=1,3,6,3,9,18$ and

$$\begin{aligned}U^{op}_c(1)=&-8\sum_{p>1}A^p\Delta^p\Big\{\int d^3r_2h^c(1,2)f^p(r_{12})f^c(r_{12})\\&\times[-\rho_0(1,2)+N^c_{cc}(1,2)]^2C_d(2)+\int d^3r_2\\&\times\int d^3r_3g^c_{cc}(1,2)g^c_{cc}(1,3)h^c(2,3)f^p(r_{23})f^c(r_{23})\\&\times[-\rho_0(2,3)+N^c_{cc}(2,3)]C_d(2)C_d(3)\Big\},\end{aligned} \quad (22)$$

with $g^c_{cc}(i,j)=[f^c(r_{ij})]^2h^c(i,j)[-\rho_0(i,j)+N^c_{cc}(i,j)]$.

The vertex corrections of the nodal equations, V^{qr}_{xy}, can be expressed in terms of the OBD and of the U functions. For the central, $p=1$ chains we have $V^{qr=11}_{dd}(i)=\rho_1(i)$ and $V^{qr=11}_{de,ed,ee,cc}(i)=C_d(i)[1+U^{op}_d(i)]$. As far as the $p>1$ chains are concerned, we insert central vertex corrections only: $V^{qr}_{dd}(i)=\rho^c_1(i)$ and $V^{qr}_{de,ed,ee,cc}(i)=C_d(i)$.

III. ENERGY EXPECTATION VALUE

In order to evaluate $\langle H\rangle$, we use the Jackson-Feenberg identity [25] for the kinetic energy, with the result

$$\langle T\rangle=T_{JF}=T_\phi+T_F, \quad (23)$$

with

$$T_\phi=-A\frac{\hbar^2}{4m}\langle\Phi^*G^2\nabla^2_1\Phi-(\nabla_1\Phi^*)G^2(\nabla_1\Phi)\rangle \quad (24)$$

and

$$T_F=-A\frac{\hbar^2}{4m}\langle\Phi^*[G\nabla^2_1G-\nabla_1G\cdot\nabla_1G]\Phi\rangle, \quad (25)$$

where $G=\mathcal{S}\Pi F_{ij}$. In turn, T_ϕ is written as

$$T_\phi=T^{(1)}_\phi+T^{(2)}_\phi+T^{(3)}_\phi. \quad (26)$$

The $T^{(n)}_\phi$ terms correspond to contributions where the kinetic energy operator acts on a nucleon not involved in any exchange ($n=1$) or belonging to a two-body ($n=2$) or to a many-body ($n=3$) exchange loop.

For $T^{(1)}_\phi$ we obtain

$$T^{(1)}_\phi=-\frac{\hbar^2}{4m}\int d^3r_1\rho_{T1}(\mathbf{r}_1)C_d(\mathbf{r}_1)[1+U^{op}_d(\mathbf{r}_1)] \quad (27)$$

and $\rho_{T1}(\mathbf{r}_1)$ is given in CO1.

For the remaining parts of T_{JF}, as well as for the two-body potential energy $\langle v\rangle=V_2$, we are faced with computing the expectation values of specific two-body operators (apart a small three-body term, in $T^{(3)}_\phi$, which will be discussed separately).

We start with $T_F+V_2=W$, also called the *interaction energy* in PW, and define $H^{ijk}_{JF}(r_{12})$ as

$$\begin{aligned}H^{ijk}_{JF}(r_{12})=&-\frac{\hbar^2}{2m}\delta_{j1}\{f^i(r_{12})\nabla^2f^k(r_{12})-\nabla f^i(r_{12})\cdot\nabla f^k(r_{12})\}\\&+f^i(r_{12})v^j(r_{12})f^k(r_{12}).\end{aligned} \quad (28)$$

In FHNC-SOC theory, W is split into four parts,

$$W=W_0+W_s+W_c+W_{cs}, \quad (29)$$

where W_0 is the sum of the diagrams with only central chains between the interacting points (IP's), connected by H_{JF}. W_s sums diagrams having SOR's touching the IP's and central chains; W_c contains diagrams with one SOC between the IP's and W_{cs} contains both SOR's at the IP's and SOC's between them.

W_0 is given by

$$W_0=\frac{1}{2}\int d^3r_1\int d^3r_2 H^{ijk}_{JF}(r_{12})h^c(1,2)(K^{ijk}A^k\{\rho^c_1(1)\rho^c_1(2)+\rho^c_1(1)C_d(2)N^c_{de}(1,2)+C_d(1)\rho^c_1(2)N^c_{ed}(1,2)+C_d(1)C_d(2)$$
$$\times[N^c_{ee}(1,2)+N^c_{ed}(1,2)N^c_{ed}(1,2)]\}-4K^{ijl}K^{lkm}A^m\Delta^m C_d(1)C_d(2)[N^c_{cc}(1,2)-\rho_0(1,2)]^2). \quad (30)$$

A sum over repeated indices is understood and the matrix K^{ijk} is given in PW.

The presence of W_s is due to the noncommutativity of the correlations. In nuclear matter and for state-independent correlations, this term is absent because of the complete cancellation of the separable diagrams (see PW for a more complete discussion of this point). We obtain

$$W_s=\frac{1}{2}\int d^3r_1\int d^3r_2 H^{ijk}_{JF}(r_{12})h^c(1,2)\left\{K^{ijk}A^k\left(1+\frac{D_{il}+D_{jl}+D_{kl}}{4}\right)([\rho^c_1(2)+C_d(2)N^c_{de}(1,2)][\rho^c_1(1)M^l_d(1)+C_d(1)M^l_e(1)]\right.$$
$$+\{\rho^c_1(2)N^c_{ed}(1,2)+C_d(2)[N^c_{ee}(1,2)+N^c_{ed}(1,2)N^c_{de}(1,2)]\}C_d(1)M^l_d(1)+[\rho^c_1(2)+C_d(2)N^c_{de}(1,2)]C_d(1)$$
$$\left.\times[2M^l_{c1}(1)+M^l_{c2}(1)])-4K^{ijl}K^{lkm}A^m\Delta^m\left(1+\frac{D_{jn}+D_{mn}+2D_{ln}}{4}\right)C_d(1)C_d(2)[N^c_{cc}(1,2)-\rho_0(1,2)]^2M^n_d(1)+1\rightleftharpoons 2\right\}. \quad (31)$$

D_{ij} are given in Eq. (5.23) of PW and we consider only terms linear in the M^l_x vertex corrections, taken of the simplified form

$$M^{l>1}_d=A^l\int d^3r_2[f^l(r_{12})]^2h^c(1,2)\{\rho^c_1(2)+C_d(2)N^c_{de}(1,2)\}, \quad (32)$$

$$M^{l>1}_e=A^l\int d^3r_2[f^l(r_{12})]^2h^c(1,2)\{\rho^c_1(2)N^c_{ed}(1,2)+C_d(2)[N^c_{ee}(1,2)+N^c_{de}(1,2)N^c_{ed}(1,2)]\}, \quad (33)$$

$$M^{l>1}_{c1}=-4A^l\Delta^l\int d^3r_2 f^c(r_{12})f^l(r_{12})h^c(1,2)C_d(2)[N^c_{cc}(1,2)-\rho_0(1,2)]^2, \quad (34)$$

$$M^{l>1}_{c2}=-4A^l\int d^3r_2[f^l(r_{12})]^2h^c(1,2)C_d(2)[N^c_{cc}(1,2)-\rho_0(1,2)]^2. \quad (35)$$

Contributions from SOC's have not been inserted into M^l_x. In W_c we must keep track of the order of the operators both in the IP's and in the SOC's. Its expression is quite lengthy and it is given in the Appendix. Because of the large number of involved operators, W_{cs} is the messiest term among all, and the smallest: so we approximate $W^j_{cs}\sim W^j_c[W^j_s/W^j_0]$, where the j index refers to the j component of H^{ijk}_{JF}. A more involved factorization approximation to W_{cs} was used in PW and its validity was set to within ~ 0.2 MeV. We have checked our approximation against the PW one in nuclear matter and found agreement up to the second decimal digit.

The decomposition (29) can be carried on also for $T^{(2)}_\phi$ and $T^{(3,2)}_\phi$ (the two-body part of $T^{(3)}_\phi$). The result is

$$T^{(2)}_{\phi,0}=-\frac{\hbar^2}{m}\int d^3r_1\int d^3r_2\rho_{T2}(1,2)C_d(1)\{K^{ikl}A^l\Delta^l C_d(2)[f^i(r_{12})f^k(r_{12})h^c(1,2)-\delta_{i1}\delta_{k1}]+C_d(2)-1\}, \quad (36)$$

$$T^{(3,2)}_{\phi,0}=-2\frac{\hbar^2}{m}\int d^3r_1\int d^3r_2\rho_{T3}(1,2)C_d(1)\{K^{ikl}A^l\Delta^l C_d(2)N^c_{cc}(1,2)[f^i(r_{12})f^k(r_{12})h^c(1,2)-\delta_{i1}\delta_{k1}]+C_d(2)$$
$$\times[N^c_{xx}(1,2)+N^c_{\rho x}(1,2)]+[C_d(2)-1][N^c_{x\rho}(1,2)+N^c_{\rho\rho}(1,2)]\}, \quad (37)$$

$$T^{(2)}_{\phi,s}=-\frac{\hbar^2}{m}\int d^3r_1\int d^3r_2\rho_{T2}(1,2)C_d(1)\left\{K^{ikl}A^l\Delta^l\left(1+\frac{D_{im}+D_{km}+D_{lm}}{4}\right)C_d(2)[f^i(r_{12})f^k(r_{12})h^c(1,2)-\delta_{i1}\delta_{k1}]\right.$$
$$\left.\times[M^m_d(1)+M^m_d(2)]+U^{op}_d(1)[C_d(2)-1]+C_d(1)U^{op}_d(2)\right\}, \quad (38)$$

$$T^{(3,2)}_{\phi,s}=-2\frac{\hbar^2}{m}\int d^3r_1\int d^3r_2\rho_{T3}(1,2)C_d(1)\left\{K^{ikl}A^l\Delta^l\left(1+\frac{D_{im}+D_{km}+D_{lm}}{4}\right)C_d(2)N^c_{cc}(1,2)[f^i(r_{12})f^k(r_{12})h^c(1,2)-\delta_{i1}\delta_{k1}]\right.$$
$$\left.\times[M^m_d(1)+M^m_d(2)]+C_d(2)N^c_{cc}(1,2)[U^{op}_d(1)+U^{op}_d(2)]-U^{op}_d(1)[N^c_{x\rho}(1,2)+N^c_{\rho\rho}(1,2)]\right\}. \quad (39)$$

$\rho_{T2,3}$ are defined in CO1. Again we give $T^{(2)}_{\phi,c}$ and $T^{(3,2)}_{\phi,c}$ in the Appendix and the cs terms are evaluated according to the approximation used for W_{cs}.

A three-body term $T^{(3,3)}_{\phi}$ originates from $\nabla_1\Phi^*\cdot\nabla_1\Phi$ in Eq. (24). It was not computed in CO1 because it is known to provide a small contribution in nuclear matter [10]. Here we include it, adopting the Kirkwood superposition approximation (KSA) for the three-body distribution functions [26] and considering only the $p=1$ correlations contribution. Following these prescriptions, we obtain

$$T^{(3,3)}_{\phi}=-2\frac{\hbar^2}{m}\int d^3r_1\int d^3r_2\int d^3r_3\nabla_1\rho_0(1,2)\cdot\nabla_1\rho_0(1,3)C_d(1)(C_d(2)C_d(3)g^c_{dd}(1,2)g^c_{dd}(1,3)$$
$$\times\{[g^c_{dd}(2,3)-1][N^c_{cc}(2,3)-\rho_0(2,3)]+N^c_{xx}(2,3)\}+\{C_d(2)g^c_{dd}(1,2)N^c_{x\rho}(2,3)[g^c_{dd}(1,3)C_d(3)-1]+2\rightleftharpoons3\}$$
$$+[N^c_{\rho\rho}(2,3)-\rho_0(2,3)][g^c_{dd}(1,3)C_d(3)-1][g^c_{dd}(1,2)C_d(2)-1]), \quad (40)$$

where $g^c_{dd}(i,j)=[f^c(r_{ij})]^2h^c(i,j)$.

IV. RESULTS

All the results presented in this section have been obtained with the single particle wave functions $\phi_\alpha(i)$ generated by a harmonic oscillator well with oscillator length $b=\sqrt{\hbar/m\omega}$. In principle, b could be considered as a variational parameter; however, we kept it fixed, at $b=1.543$ fm for ^{16}O and $b=1.654$ fm for ^{40}Ca, because our aim here is to develop and assess the finite nuclei FHNC-SOC theory, rather than to perform a fully variational calculation, to be compared with experimental data. This problem will be tackled when the complete, realistic Hamiltonian will be within reach of our approach.

The best choice for the correlation operator F_{ij} is obtained by the free minimization of the FHNC-SOC energy functional and the solution of the corresponding Euler equations $[\delta\langle H\rangle/\delta F_{ij}=0]$. This method is not practicable for realistic NN potentials and one has to resort to less ambitious ones. In CO1 two types of correlations were investigated: a simple, two-parameter Gaussian $f_G(r)$ and a more effective *Euler* function $f_{\rm Eul}(r)$, obtained by minimizing the energy evaluated at the lowest order of the cluster expansion, $\langle H_2\rangle$. The latter was also adopted in the nuclear matter studies of PW. Here we shall use the Euler correlation corresponding to Eq. (5), thus extending to the state-dependent, finite system case the approach of CO1 and PW.

Without going into many details, the correlation is computed in the (T,α) channels, with $\alpha=(S,t)$, where T and S denote the total isospin and spin of the pair and t the tensor part ($S=1$ for the t channel). In the $S=0$ case, $f_{T0}(r)$ is the solution of the Schrödinger-like equation

$$-\frac{\hbar^2}{m}\nabla^2F_{T0}(r_{12})+[\overline{V}_{T0}(r_{12})-\lambda_{T0}]F_{T0}(r_{12})=0, \quad (41)$$

where $F_{T\alpha}(r_{12})=f_{T\alpha}(r_{12})\overline{P}^{1/2}_{TS}(r_{12})$,

$$P_{TS}(1,2)=\rho_0(1)\rho_0(2)-16\rho_0^2(1,2)(-)^{T+S}, \quad (42)$$

$$Q_{TS}(1,2)=\frac{1}{2}v_{TS}(r_{12})P_{TS}(1,2)+\frac{\hbar^2}{m}\rho_{T2}(1,2)(-)^{T+S}, \quad (43)$$

and

$$\overline{V}_{TS}(r_{12})=\frac{1}{4\overline{P}_{TS}(r_{12})}\left\{2\overline{Q}_{T2}(r_{12})+\frac{\hbar^2}{4m}\right.$$
$$\left.\times\left(\nabla^2\overline{P}_{TS}(r_{12})-\frac{[\nabla\overline{P}_{TS}(r_{12})]^2}{\overline{P}_{TS}(r_{12})}\right)\right\}. \quad (44)$$

$\overline{X}_{TS}(r_{12})$, with $X=(Q,P)$, is defined as in Eq. (3.10) of CO1.

The $S=1$ correlations are solutions of two coupled equations

$$-\frac{\hbar^2}{m}\nabla^2F_{T1}(r_{12})+[\overline{V}_{T1}(r_{12})-\lambda_{T1}]F_{T1}(r_{12})$$
$$+8[v_{Tt}(r_{12})-\lambda_{Tt}]F_{Tt}(r_{12})=0 \quad (45)$$

and

$$-\frac{\hbar^2}{m}\nabla^2F_{Tt}(r_{12})$$
$$+\left[\overline{V}_{T1}(r_{12})-2v_{Tt}(r_{12})+\frac{\hbar^2}{m}\frac{6}{r_{12}^2}+2\lambda_{Tt}-\lambda_{T1}\right]F_{Tt}(r_{12})$$
$$+[v_{Tt}(r_{12})-\lambda_{Tt}]F_{T1}(r_{12})=0. \quad (46)$$

These equations are solved under the healing conditions $f_{TS}(r\geqslant d_{TS})=1$, $f_{Tt}(r\geqslant d_{Tt})=0$, and $f'_{T\alpha}(r=d_{T\alpha})=0$, where $d_{T\alpha}$ play the role of variational parameters. The $f^p(r)$ correlation functions are then obtained by $f_{T\alpha}(r)$ (see PW).

In nuclear matter only two healing distances are used: d_c and d_t, for the central (d_{TS}) and tensor (d_{Tt}) channels, respectively. We make here the same choice. Additional nuclear matter variational parameters are the quenching factors α^p of the NN potentials in the Euler equations. As in PW, we take $\alpha^1=1$ and $\alpha^{p>1}=\alpha$. We have already stated that, for the time being, we are not interested in a full variational search, and so we have taken the nuclear matter parameters given in Ref. [11] for U14. They are $d_c=2.15$ fm, $d_t=3.43$ fm, and $\alpha=0.8$.

The ^{40}Ca correlation functions are shown in Fig. 1 and compared with the corresponding nuclear matter functions,

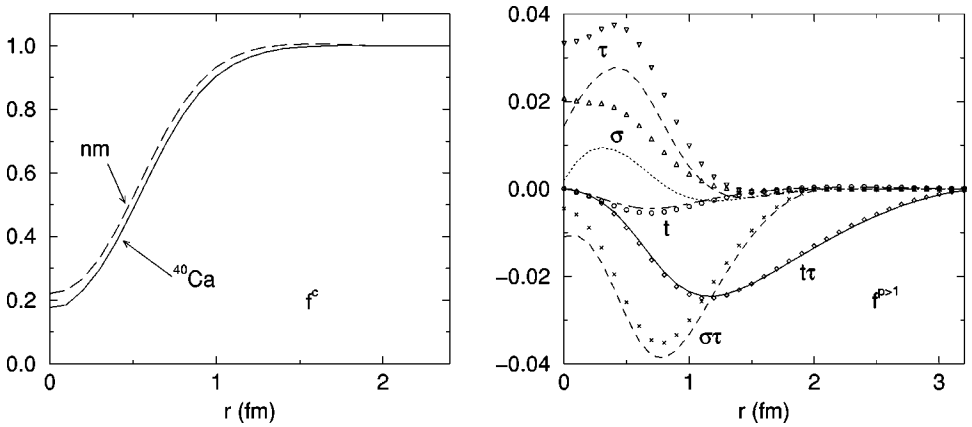

FIG. 1. Euler correlation functions in ^{40}Ca and nuclear matter (nm) at saturation density. In the right panel, lines are the ^{40}Ca correlations and symbols are the nm ones.

at saturation density. They are similar, especially the longer ranged tensor ones. The most visible differences are found in the σ and τ components and in the shortest range part of f^c. We stress that additional differences could arise from the minimization process, as the energy minimum will probably correspond to a different choice of the parameters.

A measure of the accuracy of the FHNC-SOC approximation is how well the densities normalization sum rules are satisfied:

$$S_1 = \int d^3r_1 \rho_1(\mathbf{r}_1) = A, \tag{47}$$

$$S_2 = \frac{1}{A(A-1)} \int d^3r_1 \int d^3r_2 \rho_2^c(\mathbf{r}_1, \mathbf{r}_2) = 1, \tag{48}$$

$$S_\tau = \frac{1}{3A} \int d^3r_1 \int d^3r_2 \rho_2^\tau(\mathbf{r}_1, \mathbf{r}_2) = -1. \tag{49}$$

The spin saturation sum rule $S_\sigma = -1$, holds only in the absence of tensor correlations [27]. Both the TBD and its sum rules are evaluated following the decomposition (29).

Deviations of the sum rules from their exact values are due to (i) the FHNC/0 scheme and (ii) the SOC approximation. The influence of the elementary diagrams was addressed in CO1. It was found that $E_{ee}^{\rm exch}$, i.e., the sum of the *ee* elementary diagrams whose external points belong to the same exchange loop, may substantially contribute to both S_τ and to the potential energy, if the potential has large exchange terms. This fact can be understood if we consider that a four-point elementary diagram, linear in the central link, $[f^c]^2-1$, is contained in $E_{ee}^{\rm exch}$, as well as diagrams linear in the operatorial link $f^c f^{l>1}$. The insertion of these diagrams in the FHNC equations was termed as the FHNC-1 approximation, and we shall keep this terminology.

Results for the sum rules are presented in Table I for different models of the correlation: f^c (Jastrow, $p=1$ component only) and f^4 and f^6 (without and with tensor correlations, respectively). The table shows also the FHNC-1 corrections. In all cases, S_1 shows a largest error of less than 1%. This is also the accuracy that we find in the Jastrow case for $S_{2,\tau}$, in the FHNC-1 approximation, as already noticed in CO1. The situation is worst for the operatorial correlations, where FHNC-SOC theory violates the sum rules by a maximum amount of $\sim 9\%$, similar to what was already found in nuclear matter in Ref. [10].

TABLE I. ^{16}O and ^{40}Ca sum rules for U14 with different correlations. The f^c line corresponds to the Jastrow model; the $f^{6(4)}$ line gives results with (without) tensor correlations. Numbers in parentheses are obtained in the FHNC-1 approximation.

		S_1	S_2	S_τ
^{16}O	f^c	16.00	0.998 (1.002)	−1.057 (−1.001)
	f^4	16.03	0.988 (1.001)	−0.980 (−0.965)
	f^6	16.01	1.051 (1.054)	−0.943 (−0.930)
^{40}Ca	f^c	40.00	0.999 (1.001)	−1.067 (−1.002)
	f^4	40.03	1.005 (1.007)	−1.074 (−1.056)
	f^6	39.86	1.089 (1.091)	−0.997 (−0.981)

TABLE II. Contributions to the energy per nucleon, in MeV, for ^{16}O with the truncated U14 potential, the $p=1$, Jastrow part of the Euler correlation, and the harmonic oscillator single particle wave functions discussed in the text. The $E_{ee}^{\rm exch}$ column gives the FHNC-1 correction.

		0	$+s$	$+c$	$+cs$	$+E_{ee}^{\rm exch}$	CMC
$T_\phi^{(1)}$	14.32						
$T_\phi^{(2)}$		3.90					
$T_\phi^{(3,2)}$		0.73					
$T_\phi^{(3,3)}$	0.07						
T_F		5.59					
$\langle T \rangle$		24.61					24.33(21)
$\langle v^c \rangle$		0.84				0.88	0.93(28)
$\langle v^\sigma \rangle$		1.28				1.25	1.27(08)
$\langle v^\tau \rangle$		2.46				2.40	2.43(12)
$\langle v^{\sigma\tau} \rangle$		−27.34				−26.59	−26.24(26)
$\langle v_2 \rangle$		−22.76				−22.07	−21.56(25)
$\langle H \rangle / A$		1.78				2.54	2.77(09)
$T_{\rm c.m.}/A$	0.82						
$E_{\rm g.s.}/A$						1.72	

TABLE III. As in Table II, for the f^4 correlation model.

		0	$+s$	$+c$	$+cs$	$+E_{ee}^{\rm exch}$	CMC
$T_\phi^{(1)}$	14.41						
$T_\phi^{(2)}$		4.98	4.97	4.97	4.97		
$T_\phi^{(3,2)}$		1.44	1.44	0.05	0.05		
$T_\phi^{(3,3)}$	0.07						
T_F		8.09	8.28	7.80	7.79		
$\langle T\rangle$		29.00	29.17	27.30	27.29		26.15(31)
$\langle v^c\rangle$		3.04	3.13	2.43	2.41	2.41	2.72(37)
$\langle v^\sigma\rangle$		2.27	2.26	2.07	2.07	2.02	2.07(10)
$\langle v^\tau\rangle$		2.38	2.35	2.35	2.35	2.28	2.40(12)
$\langle v^{\sigma\tau}\rangle$		−34.42	−34.56	−32.82	−32.81	−32.10	−31.76(33)
$\langle v_2\rangle$		−26.73	−26.82	−25.96	−25.98	−25.39	−24.58(29)
$\langle H\rangle/A$		2.26	2.36	1.34	1.31	1.90	1.57(09)
$T_{\rm c.m.}/A$	0.82						
$E_{\rm g.s.}/A$						1.08	

The ground state energies are displayed in Tables II–IV for ^{16}O and Tables V–VII for ^{40}Ca, for each correlation model. The columns $(0,s,c,cs)$ show the contributions to the two-body operator expectation values, as given in Eq. (29). The ^{16}O results are compared with the calculations of Pieper [28] with the cluster Monte Carlo (CMC) method of Ref. [7]. As already outlined, in the CMC approach the Jastrow part of the correlation is exactly treated by MC sampling and the remaining operatorial contributions are evaluated by the MC method up to four-nucleon clusters. The fourth order cluster expansion seems to be enough to provide a reliable convergence and to consider the CMC numbers as a benchmark for FHNC theory. The tables also contain the FHNC-1 corrections.

The ground state energy mean value $E_{\rm g.s.}$ is then given by $E_{\rm g.s.}=\langle H\rangle-T_{\rm c.m.}$, where $T_{\rm c.m.}$ is the center-of-mass kinetic energy, whose calculation is discussed in CO1.

For the Jastrow correlation, FHNC theory shows an error of 1–2 % for $\langle T\rangle$ and $\langle v_2\rangle$ in ^{16}O. The total energy percentile error is bigger ($\sim$9%) as $\langle H\rangle$ is given by the cancellation of two large numbers. We meet the same situation in the f^4 and f^6 models. The kinetic and potential energy errors are 3–4 % in the first case and 5–7 % in the latter. The absolute error in $\langle H\rangle$ is considerably less than 1 MeV in all models. Again, this finding is consistent with the estimated accuracy of FHNC-SOC theory in nuclear matter. We notice that most of the binding is given by the OPE parts of the potential, $v^{\sigma\tau}$ and $v^{t\tau}$. In absence of the last component, ^{16}O is not bound

TABLE IV. As in Table II, for the f^6 correlation model.

		0	$+s$	$+c$	$+cs$	$+E_{ee}^{\rm exch}$	CMC
$T_\phi^{(1)}$	14.75						
$T_\phi^{(2)}$		5.04	4.95	4.93	4.93		
$T_\phi^{(3,2)}$		1.33	1.29	−0.04	0.00		
$T_\phi^{(3,3)}$	0.07						
T_F		11.45	12.22	11.46	11.41		
$\langle T\rangle$		32.63	33.28	31.16	31.16		29.45(33)
$\langle v^c\rangle$		3.03	3.31	2.41	2.33	2.33	2.35(43)
$\langle v^\sigma\rangle$		2.17	2.13	2.02	2.02	1.97	2.00(13)
$\langle v^\tau\rangle$		2.34	2.26	2.36	2.36	2.29	2.23(14)
$\langle v^{\sigma\tau}\rangle$		−33.79	−34.25	−32.71	−32.69	−32.03	−30.12(42)
$\langle v^t\rangle$		0.31	0.30	0.26	0.26	0.25	0.27(01)
$\langle v^{t\tau}\rangle$		−11.42	−11.82	−10.41	−10.36	−10.28	−9.77(09)
$\langle v_2\rangle$		−37.37	−38.07	−36.07	−36.08	−35.47	−33.03(31)
$\langle H\rangle/A$		−4.74	−4.80	−4.91	−4.92	−4.33	−4.59(10)
$T_{\rm c.m.}/A$	0.82						
$E_{\rm g.s.}/A$						−5.15	

TABLE V. As in Table II, for ^{40}Ca.

		0	$+s$	$+c$	$+cs$	$+E_{ee}^{\text{exch}}$
$T_\phi^{(1)}$	14.81					
$T_\phi^{(2)}$		5.00				
$T_\phi^{(3,2)}$		1.74				
$T_\phi^{(3,3)}$	0.72					
T_F		8.29				
$\langle T\rangle$		30.55				
$\langle v^c\rangle$		−1.45				−1.41
$\langle v^\sigma\rangle$		1.60				1.57
$\langle v^\tau\rangle$		3.06				2.99
$\langle v^{\sigma\tau}\rangle$		−33.30				−32.40
$\langle v_2\rangle$		−30.09				−29.26
$\langle H\rangle/A$		0.47				1.30
$T_{\text{c.m.}}/A$	0.28					
$E_{\text{g.s.}}/A$						1.01

in our model. The same holds in ^{40}Ca, where the introduction of tensor correlations and potentials increases the kinetic energy by $\sim$5.6 MeV, compensated by an additional potential energy contribution of ~ -13.6 MeV, providing a bound nucleus in the f^6 case. For the sake of curiosity, we recall that the experimental binding energies per nucleon are -7.72 MeV in ^{16}O and -8.30 MeV in ^{40}Ca, to be compared with the computed values $E_{\text{g.s.}}=-5.15$ MeV (^{16}O) and -7.87 MeV (^{40}Ca).

In Table VIII we compare the expectation values of the components of the potential with the nuclear matter results, within the same FHNC-SOC approximation and in the f^6 model. It is interesting to notice a kind of convergence with A for the potential energies, in particular for the large OPE-related components, whose contributions, in ^{40}Ca, are already very close to the nuclear matter values. We stress that

TABLE VI. As in Table V, for the f^4 correlation model.

		0	$+s$	$+c$	$+cs$	$+E_{ee}^{\text{exch}}$
$T_\phi^{(1)}$	14.92					
$T_\phi^{(2)}$		6.06	6.06	6.06	6.06	
$T_\phi^{(3,2)}$		2.74	2.75	1.05	1.04	
$T_\phi^{(3,3)}$	0.73					
T_F		11.72	12.08	11.39	11.37	
$\langle T\rangle$		36.17	36.54	34.15	34.12	
$\langle v^c\rangle$		1.16	1.21	0.18	0.14	0.14
$\langle v^\sigma\rangle$		2.78	2.77	2.45	2.45	2.38
$\langle v^\tau\rangle$		2.94	2.90	2.83	2.83	2.74
$\langle v^{\sigma\tau}\rangle$		−42.69	−42.92	−39.78	−39.76	−38.92
$\langle v_2\rangle$		−35.80	−36.04	−34.33	−34.34	−33.66
$\langle H\rangle/A$		0.36	0.49	−0.18	−0.22	0.46
$T_{\text{c.m.}}/A$	0.28					
$E_{\text{g.s.}}/A$						0.18

TABLE VII. As in Table V, for the f^6 correlation model.

		0	$+s$	$+c$	$+cs$	$+E_{ee}^{\text{exch}}$
$T_\phi^{(1)}$	15.37					
$T_\phi^{(2)}$		6.12	6.07	6.07	6.07	
$T_\phi^{(3,2)}$		2.50	2.49	0.92	0.93	
$T_\phi^{(3,3)}$	0.70					
T_F		16.27	15.63	16.66	16.62	
$\langle T\rangle$		40.96	42.47	39.72	39.69	
$\langle v^c\rangle$		1.13	1.29	−0.03	−0.22	−0.21
$\langle v^\sigma\rangle$		2.61	2.54	2.35	2.35	2.30
$\langle v^\tau\rangle$		2.83	2.69	2.79	2.79	2.71
$\langle v^{\sigma\tau}\rangle$		−41.41	−42.27	−39.54	−39.48	−38.73
$\langle v^t\rangle$		0.37	0.35	0.30	0.30	0.29
$\langle v^{t\tau}\rangle$		−15.43	−16.23	−13.72	−14.22	−14.14
$\langle v_2\rangle$		−49.91	−51.61	−47.85	−48.48	−47.28
$\langle H\rangle/A$		−8.95	−9.15	−8.13	−8.79	−7.59
$T_{\text{c.m.}}/A$	0.28					
$E_{\text{g.s.}}/A$						−7.87

TABLE VIII. Breakup of the FHNC-SOC potential energies in MeV per nucleon for ^{16}O, ^{40}Ca, and nuclear matter (nm) in the f^6 model.

	^{16}O	^{40}Ca	nm
$\langle v^c\rangle$	2.33	−0.21	−3.04
$\langle v^\sigma\rangle$	1.97	2.30	2.46
$\langle v^\tau\rangle$	2.29	2.71	2.84
$\langle v^{\sigma\tau}\rangle$	−32.03	−38.73	−37.69
$\langle v^t\rangle$	0.25	0.29	0.32
$\langle v^{t\tau}\rangle$	−10.28	−14.14	−14.06
$E_{\text{g.s.}}/A$	−5.15	−7.87	−13.16

TABLE IX. Contributions in MeV to the ^{16}O energy per nucleon with and without SOR insertions and in the CMC method.

	SOC	SOC+SOR	CMC
f^4			
$\langle T\rangle$	27.29	27.25	26.15(31)
$\langle v^c\rangle$	2.41	2.00	2.72(37)
$\langle v^\sigma\rangle$	2.02	2.02	2.07(10)
$\langle v^\tau\rangle$	2.28	2.30	2.40(12)
$\langle v^{\sigma\tau}\rangle$	−32.10	−32.01	−31.76(33)
f^6			
$\langle T\rangle$	31.16	31.08	29.45(33)
$\langle v^c\rangle$	2.33	1.92	2.35(43)
$\langle v^\sigma\rangle$	1.97	1.96	2.00(13)
$\langle v^\tau\rangle$	2.29	2.30	2.23(14)
$\langle v^{\sigma\tau}\rangle$	−32.03	−31.81	−30.12(42)
$\langle v^t\rangle$	0.25	0.26	0.27(01)
$\langle v^{t\tau}\rangle$	−10.28	−10.21	−9.77(09)

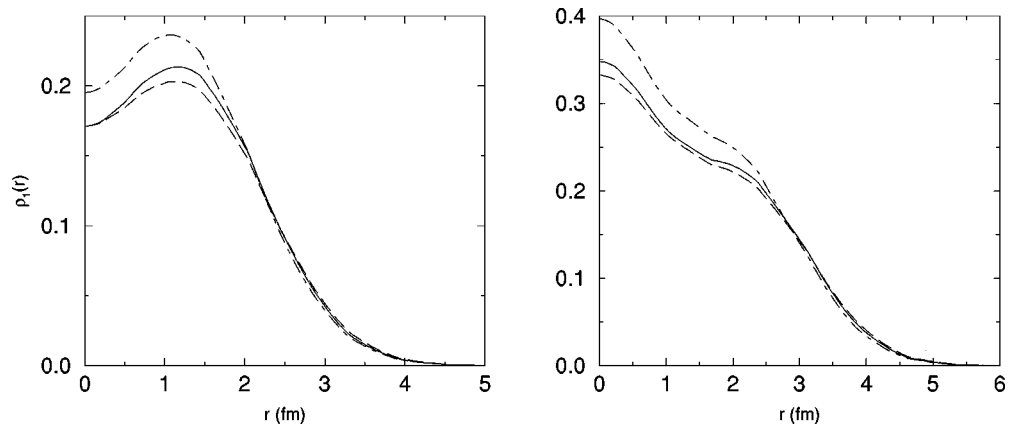

FIG. 2. One-body densities in ^{16}O (left) and ^{40}Ca (right). The solid lines correspond to the f^6 model, the dashed line to the Jastrow model, and the dot-dashed line to the IPM.

a more meaningful comparison would imply the use of Hartree-Fock single particle wave functions or, at least, a minimization on the single particle potential parameters.

In Table IX we show the influence of the SOR's in ^{16}O. SOR's have been inserted according to PW. In general, they contribute less than 1% of the FHNC-SOC value, with the exception of $\langle v^c \rangle$, where they give a 17–18 % contribution, actually worsening the agreement with the CMC method.

The effects of the correlations on the ground state structure are shown in Figs. 2 and 3, giving the OBD's and the two-particle distribution functions $\rho_2(\mathbf{r}_{12})$, defined as

$$\rho_2(\mathbf{r}_{12}) = \frac{1}{A} \int d^3R_{12} \rho_2^c(\mathbf{r}_1, \mathbf{r}_2), \tag{50}$$

where $\mathbf{R}_{12} = \frac{1}{2}(\mathbf{r}_1 + \mathbf{r}_2)$ is the center-of-mass coordinate. In both figures, the f^6, the Jastrow, and the independent particle models are compared

A large part of the reduction with respect to the IPM is due to the Jastrow, short range correlations. The operatorial correlations slightly enhance the OBD's, as in the first order cluster analysis of Ref. [19]. They have the same effect in $\rho_2(\mathbf{r}_{12})$, where the dip at short distances is due to the repulsive core in the nuclear interaction, as already found for $A=3,4$ nuclei in Ref. [29].

At the beginning of this section we have explained why we did not look for a variational minimum for the truncated version of U14. However, it is certainly of interest to try to understand how reliable are the nuclear matter parameter values and how far they are from the true minimum. To this aim we have minimized, with respect to d_c, the energy for the $S3$ model described in the Introduction (keeping the same harmonic oscillator wells as U14). The results are displayed in Table X. The first row corresponds to the U14 nuclear matter $d_c = 2.15$ fm, whereas the second gives the computed minima. The minimization produces a small gain in the binding energy and $S3$ appears to provide two nuclei underbound of ~ 1 MeV.

V. CONCLUSIONS

In this article the FHNC technology developed in CO1 to describe finite nuclear systems has been extended to state-dependent correlations containing up to tensor components. As in infinite nucleon matter, the noncommutativity of the two-body correlation operators does not allow for a complete FHNC treatment, which is instead possible for purely scalar, Jastrow-type correlations. The single operator chain approximation scheme (which is effectively employed in nuclear and neutron matter) has been extended to the finite case. The resulting set of integral equations has been solved either by neglecting the class of the elementary diagrams (FHNC/0 approximation) or by considering only the lowest order elementary contribution in the dynamical correlation (FHNC-

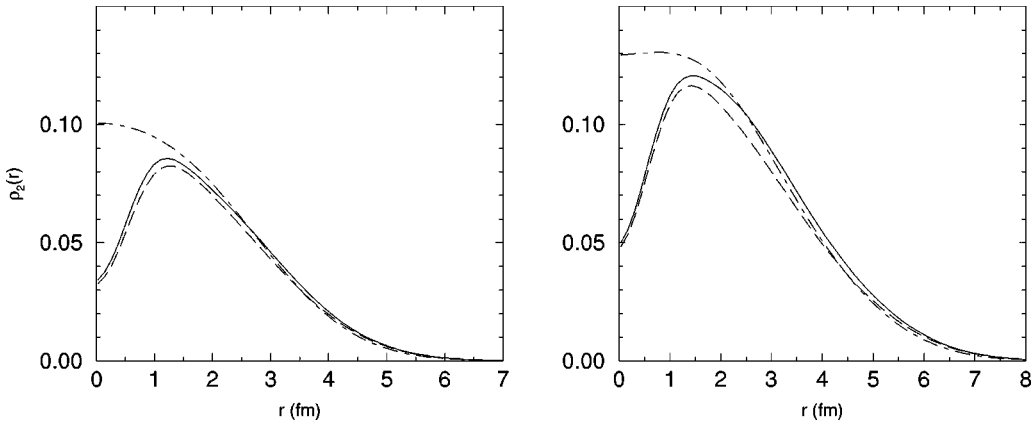

FIG. 3. Two-particle distribution functions in ^{16}O (left) and ^{40}Ca (right). As in Fig. 2.

TABLE X. Energies per nucleon (in MeV) and central healing distances (in fm) for the $S3$ interaction in the f^4 model.

^{16}O	d_c	$E_{\text{g.s.}}/A$	^{40}Ca	d_c	$E_{\text{g.s.}}/A$
	2.15	−6.08		2.15	−7.37
	1.96	−6.27		2.02	−7.50

1). As an application, we have studied the ground state properties of the doubly closed shell nuclei in the ls coupling scheme, ^{16}O and ^{40}Ca, interacting by the central and tensor components of the realistic Urbana v_{14} nucleon-nucleon potential.

The analysis of the sum rules shows that the FHNC-SOC equations provide a considerably accurate one-body density, whose normalization is violated by much less than 1%. A comparably good accuracy is obtained for the normalization of the central component of the two-body density ($S_2=1$ sum rule) when tensor correlations are not included. If they are considered, then the excellent fulfillment of S_2 obtained with purely central correlations slightly worsens. The inclusion of the first order Jastrow elementary diagram in the FHNC-1 approximation does not improve the outcome. Inclusion of analogous diagrams, linear in the operatorial correlations, is presently under consideration. In any case, the worst violation of the sum rule is $\sim 9\%$, close to what was found in nuclear matter. A similar situation is met for the isospin saturation, $S_\tau=-1$, sum rule.

The various energy contributions in ^{16}O have been compared with those obtained within the cluster Monte Carlo approach. The maximum disagreement with the CMC results varies from $\sim 2\%$ for the Jastrow model to $\sim 7\%$ for the tensor model. The absolute error in the ground state energy per nucleon is always well less 1 MeV, compatible with the estimated accuracy of the FHNC-SOC approach in nuclear matter at saturation density.

The same truncated v_{14} interaction has been also used to study the ground state of ^{40}Ca. We have verified that for both ^{16}O and ^{40}Ca only the insertion of the long-range one-pion exchange parts of the potential (and related correlations) binds the nuclei.

No minimization along the correlation and single particle potential variational parameters has been carried on, but we have rather taken the nuclear matter values. We have postponed this task to future works, when a completely realistic Hamiltonian will be within reach of our method. However, a partial minimization on the correlation healing distance d_c for the simpler, central Afnan-Tang potential seems to point to little variation of the parameters in going from the infinite to the finite case.

Even if this is still an intermediate step towards a full microscopic description of intermediate and heavy nuclei, our results are very promising. In fact, we may conclude that the FHNC-SOC approach to finite nuclei shows at least the same degree of accuracy estimated in the best variational nuclear matter studies. In this respect, we consider as mandatory the inclusion of spin-orbit terms in both the interaction and correlation, as well as the extension to the jj coupling scheme, in order to cover all the range of the doubly closed shell nuclei.

ACKNOWLEDGMENTS

The authors are deeply indebted to Steven Pieper for providing the CMC results in ^{16}O.

APPENDIX

In this appendix we give the W_c, $T^{(2)}_{\phi,c}$, and $T^{(3,2)}_{\phi,c}$ expressions. W_c is given by the sum

$$W_c = W_c(dd) + W_c(de) + W_c(ed) + W_c(ee) + W_c(cc), \tag{A1}$$

with

$$\begin{aligned} W_c(dd) = \frac{1}{2}\int d^3r_1 \int d^3r_2 H^{ijk}_{JF}(r_{12}) h^c(1,2) N^{l>1}_{dd}(1,2) \Bigg\{ & \{\rho^c_1(1)\rho^c_1(2) + \rho^c_1(1) C_d(2) N^c_{de}(1,2) + C_d(1)\rho^c_1(2) N^c_{ed}(1,2) \\ & + C_d(1) C_d(2)[N^c_{ee}(1,2) + N^c_{ed}(1,2) N^c_{ed}(1,2)]\} \frac{1}{24}(11 K^{ijm} K^{klm} A^m + 5 K^{ijm} L^{klm} + 5 K^{jkm} L^{ilm} + 3 K^{ikm} L^{jlm}) \\ & - 4 C_d(1) C_d(2)[N^c_{cc}(1,2) - \rho_0(1,2)]^2 \Delta^n \Bigg[\frac{1}{8}(K^{jkm} K^{nim'} L^{m'lm} + K^{ijm} K^{mkm'} L^{nlm'} + K^{knm} K^{mim'} L^{jlm'} \\ & + K^{ijm} K^{knm'} L^{m'lm}) + \frac{1}{12}(4 K^{nlm} K^{ijm'} K^{mm'k} A^k + K^{jkm} K^{mnm'} L^{ilm'} + K^{nim} K^{mjm'} L^{klm'}) \Bigg] \Bigg\}, \end{aligned} \tag{A2}$$

$$\begin{aligned} W_c(de) = W_c(ed) = \frac{1}{2}\int d^3r_1 \int d^3r_2 H^{ijk}_{JF}(r_{12}) h^c(1,2) N^{l>1}_{de}(1,2) \{\rho^c_1(1) C_d(2) + C_d(1) C_d(2) N^c_{ed}(1,2)\} \\ \times \frac{1}{4}(2 K^{ijm} K^{klm} A^m + K^{ijm} L^{klm} + K^{jkm} L^{ilm}), \end{aligned} \tag{A3}$$

$$W_c(ee) = \frac{1}{2}\int d^3r_1 \int d^3r_2 H^{ijk}_{JF}(r_{12}) h^c(1,2) N^{l>1}_{ee}(1,2) C_d(1) C_d(2) K^{ijm} K^{klm} A^m, \tag{A4}$$

$$W_c(cc)=\frac{1}{2}(-8)\int d^3r_1\int d^3r_2 H^{ijk}_{JF}(r_{12})h^c(1,2)C_d(1)C_d(2)[N^c_{cc}(1,2)-\rho_0(1,2)]\Delta^n\Big\{N^{l>1}_{cc,int}(1,2)K^{jkm}K^{imm'}L^{m'nl}$$
$$+[N^{l>1}_{cc,R}(1,2)+N^{l>1}_{cc,L}(1,2)]\,\frac{1}{8}(K^{jkm}K^{mnm'}K^{im'l}A^l+K^{jkm}K^{mnm'}L^{im'l}+K^{jkm}K^{inm'}K^{mm'l}A^l$$
$$+K^{jkm}K^{inm'}L^{mm'l}+2K^{jkm}K^{imm'}L^{nm'l}+K^{ijm}K^{nmm'}L^{m'kl}+K^{ijm}K^{nkm'}L^{m'ml})\Big\}. \tag{A5}$$

In the last equation, $N^{l>1}_{cc,L(R)}$ are cc nodal functions having the X^l_{cc} link reaching the left (right) external point. $N^{l>1}_{cc,int}$ has X^l_{cc} as an internal link.

$N^{l>1}_{cc,L}$ is given by

$$N^{l>1}_{cc,L}(1,2)=N^{l>1}_{xx,L}(1,2)+N^{l>1}_{x\rho,L}(1,2), \tag{A6}$$

where $N^{l>1}_{xx,L}$ and $N^{l>1}_{x\rho,L}$ are solutions of

$$N^{l>1}_{xx,L}(1,2)=\sum_{qr}\int d^3r_3\xi^{qrl}_{132}X^q_{cc,L}(1,3)V^{qr}_{cc}(3)[X^c_{cc}(3,2)+N^c_{xx}(3,2)+N^c_{\rho x}(3,2)]\Delta^r, \tag{A7}$$

$$N^{l>1}_{x\rho,L}(1,2)=\sum_{qr}\int d^3r_3\xi^{qrl}_{132}X^q_{cc,L}(1,3)V^{qr}_{cc}(3)[-\rho_0(3,2)+N^c_{x\rho}(3,2)+N^c_{\rho\rho}(3,2)]\Delta^r, \tag{A8}$$

and

$$X^{l>1}_{cc,L}(1,2)=h^l(1,2)h^c(1,2)[N^c_{cc}(1,2)-\rho_0(1,2)]+\{[f^c(r_{12})]^2h^c(1,2)-1\}N^l_{cc,L}(1,2). \tag{A9}$$

For the other functions, we have $N^{l>1}_{cc,R}(1,2)=N^{l>1}_{cc,L}(2,1)$ and $N^{l>1}_{cc,int}=N^{l>1}_{cc}-N^{l>1}_{cc,L}-N^{l>1}_{cc,R}$.

Finally, $T^{(2)}_{\phi,c}$ and $T^{(3,2)}_{\phi,c}$ are given by

$$T^{(2)}_{\phi,c}=-\frac{\hbar^2}{m}\int d^3r_1\int d^3r_2\rho_{T2}(1,2)C_d(1)C_d(2)f^i(r_{12})f^k(r_{12})h^c(1,2)N^{l>1}_{dd}(1,2)\Delta^n$$
$$\times\left[\frac{1}{8}(K^{nim}L^{mlk}+K^{ikm}L^{nlm}+K^{knm}K^{mil}A^l+K^{knm}L^{mli})+\frac{1}{12}(4K^{nlm}K^{mik}A^k+K^{knm}L^{ilm}+K^{inm}L^{klm})\right], \tag{A10}$$

$$T^{(3,2)}_{\phi,0}=-\frac{\hbar^2}{m}\int d^3r_1\int d^3r_2\rho_{T3}(1,2)C_d(1)C_d(2)\Delta^n\Big\{2\,f^i(r_{12})f^k(r_{12})h^c(1,2)N^{l>1}_{dd}(1,2)N^c_{cc}(1,2)$$
$$\times\left[\frac{1}{8}(K^{nim}L^{mlk}+K^{ikm}L^{nlm}+K^{knm}K^{mil}A^l+K^{knm}L^{mli})+\frac{1}{12}(4K^{nlm}K^{mik}A^k+K^{knm}L^{ilm}+K^{inm}L^{klm})\right]$$
$$+[f^i(r_{12})f^k(r_{12})h^c(1,2)-\delta_{i1}\delta_{k1}]\Big[[N^{l>1}_{cc,L}(1,2)+N^{l>1}_{cc,R}(1,2)]\,\frac{1}{4}(K^{knm}K^{iml}A^l+K^{knm}L^{iml}+K^{inm}K^{kml}A^l+K^{inm}L^{kml}$$
$$+2K^{ikm}L^{nml}+K^{nim}L^{mkl}+K^{nkm}L^{mil})+N^{l>1}_{cc,int}(1,2)K^{ikm}L^{nml}\Big]\Big\}$$
$$-2\frac{\hbar^2}{m}\int d^3r_1\int d^3r_2\rho_{T3}(1,2)C_d(1)A^l\Delta^l\{C_d(2)[N^{l>1}_{xx,int}(1,2)+N^{l>1}_{\rho x,int}(1,2)]+[C_d(2)-1]N^{l>1}_{x\rho,int}(1,2)\}. \tag{A11}$$

The L^{ijk} matrix is given in PW.

[1] C. R. Chen, G. L. Payne, J. L. Friar and B. F. Gibson, Phys. Rev. C **3**, 1740 (1986); A. Stadler, W. Glöckle, and P. U. Sauer, Phys. Rev. C **44**, 2319 (1991).

[2] J. Carlson, Phys. Rev. C **38**, 1879 (1988).

[3] A. Kievsky, M. Viviani, and S. Rosati, Nucl. Phys. **A551**, 241 (1993).

[4] B. S. Pudliner, V. R. Pandharipande, J. Carlson, S. C. Pieper, and R. B. Wiringa, Phys. Rev. C **56**, 1720 (1997).

[5] A. Kievsky, M. Viviani, and S. Rosati, Nucl. Phys. **A557**, 511 (1994).

[6] R. B. Wiringa, Phys. Rev. C **43**, 1585 (1991).

[7] S. C. Pieper, R. B. Wiringa, and V. R. Pandharipande, Phys. Rev. C **46**, 1741 (1992).

[8] B. D. Day, Rev. Mod. Phys. **50**, 495 (1978); B. D. Day and R.

B. Wiringa, Phys. Rev. C **32**, 1057 (1985).
[9] M. Baldo, I. Bombaci, S. Ferreira, G. Giansiracusa, and U. Lombardo, Phys. Rev. C **43**, 2605 (1991).
[10] R. B. Wiringa, V. Ficks, and A. Fabrocini, Phys. Rev. C **38**, 1010 (1988).
[11] A. Fabrocini and S. Fantoni, Phys. Lett. B **298**, 263 (1993).
[12] M. Baldo (private communication).
[13] A. Fabrocini and S. Fantoni, Nucl. Phys. **A503**, 375 (1989).
[14] A. Fabrocini, Phys. Rev. C **55**, 338 (1997).
[15] O. Benhar, A. Fabrocini, and S. Fantoni, Nucl. Phys. **A550**, 201 (1992).
[16] G. Co', A. Fabrocini, S. Fantoni, and I. E. Lagaris, Nucl. Phys. **A549**, 439 (1992).
[17] G. Co', A. Fabrocini, and S. Fantoni, Nucl. Phys. **A568**, 73 (1994).
[18] F. Arias de Saavedra, G. Co', A. Fabrocini, and S. Fantoni, Nucl. Phys. **A605**, 359 (1996).
[19] F. Arias de Saavedra, G. Co', and M. M. Renis, Phys. Rev. C **55**, 673 (1997).
[20] I. E. Lagaris and V. R. Pandharipande, Nucl. Phys. **A359**, 331 (1981); **A359**, 349 (1981).
[21] I. R. Afnan and Y. C. Tang, Phys. Rev. **175**, 1337 (1968).
[22] S. Rosati, in *From Nuclei to Particles*, Proceedings of the International School ''Enrico Fermi,'' Course LXXIX, Varenne, 1981, edited by A. Molinari (North-Holland, Amsterdam, 1982).
[23] V. R. Pandharipande and R. B. Wiringa, Rev. Mod. Phys. **51**, 821 (1979).
[24] R. B. Wiringa, Nucl. Phys. **A338**, 57 (1980).
[25] S. Fantoni and S. Rosati, Phys. Lett. B **84**, 23 (1979).
[26] E. Feenberg, *Theory of Quantum Liquids* (Academic, New York, 1969).
[27] R. Guardiola and A. Polls, Anal. Fis. A **77**, 11 (1981).
[28] S. C. Pieper (private communication).
[29] R. Schiavilla *et al.*, Nucl. Phys. **A473**, 267 (1987).